

# Subduction megathrust locking and slip behavior: Insights from geodesy

Laura M. Wallace (University of Texas Institute for Geophysics, GNS Science, New Zealand),  
Noel Bartlow (Kansas University), Julie Elliott (Purdue University), Susan Schwartz (UC Santa Cruz)

Our understanding of subduction zone slip has been transformed over the last two decades, thanks in large part to the advent of high-precision geodetic techniques. These have illuminated crustal deformation at all stages of the earthquake cycle, as well as a rich variety of transient, aseismic slip processes. These observations have provoked new questions regarding fault mechanics and earthquake occurrence, helping to guide multi-disciplinary investigations at MARGINS and GeoPRISMS focus sites to reveal the processes behind subduction plate boundary dynamics. MARGINS and GeoPRISMS have especially played an important role in expanding geodetic investigations of subduction megathrust slip at many of its focus sites, which include Costa Rica, Nankai, Cascadia, Alaska, and New Zealand. Together, these locales exhibit virtually every known flavor of subduction slip behavior, megathrust locking characteristics, and subduction margin physical properties. Together this diversity has provided an outstanding opportunity to resolve the physical processes leading to episodic slow slip, as well as those causing some subduction zones to lock-up and slip in Great (Mw >8.0) earthquakes versus being dominated by aseismic creep processes.

## Introduction

The advent of space geodetic techniques to monitor crustal deformation has revolutionized our ability to resolve subduction megathrust slip processes at all stages of the earthquake cycle. During the time between large subduction thrust earthquakes (the interseismic period), the subducting and overriding tectonic plates can become locked together, accumulating stresses for hundreds of years or more that will ultimately be relieved in future subduction earthquakes. This “locking” or “coupling” (we use the two terms interchangeably here) creates accumulation of elastic strain in the surrounding crust, which can be measured as small changes in ground movement at the Earth’s surface above subduction zones (Fig. 1). Data from satellites that are part of the Global Positioning System (GPS) and more recently, other Global Navigation Satellite Systems (GNSS) captured by antennas mounted on geodetic monuments on the Earth’s surface enable measurement of changes of the position of these monuments, at a millimeter-level or better (hereafter, we use GPS/GNSS to refer to technologies related to GPS and GNSS). We can use these changes in surface movements to determine where and how fast the plates are locking together and accumulating stress that may be relieved in future earthquakes. In the case of some recent, major subduction earthquakes, the portions of the subduction plate interface that ruptured generally coincide with regions where the plate interface was locked prior to the earthquake, as determined by geodetic measurements (e.g., Loveless and Meade, 2011; Protti et al., 2014; Métois et al., 2016). Delineation of the locked plate interface using geodetic studies has revealed the likely seismogenic zone (e.g., the region on a fault where earthquakes

nucleate) at many subduction zones worldwide, greatly improving our understanding of earthquake and tsunami hazard posed by subduction plate boundaries. These locked regions are often located offshore, and wider use of seafloor geodetic techniques is needed to better define them.

More recently, scientists have discovered the existence of episodic slow slip events (SSEs) that occur repeatedly on subduction megathrust faults (Dragert et al., 2001; Schwartz and Rokosky, 2007 and references therein). SSEs involve a few to tens of centimeters of slip along faults over days to years, and can be likened to earthquakes in slow motion. Because SSEs occur so slowly, detecting them relies on monitoring millimeter- to centimeter-level changes in the position of the Earth’s surface above the SSEs using a range of geodetic methods. Integrating temporally diverse observations from geodesy (hours to years) and seismology (seconds to minutes) has provided further insight into SSEs and related fault slip processes. The discovery of SSEs on many subduction zones and other types of faults around the world over the last fifteen years has revealed that faults undergo slip in a broad spectrum of slip behaviors, and that these slow events play a major role in the earthquake cycle and the accommodation of plate motion. These discoveries have sparked exciting new fields of inquiry in geodesy, seismology, and fault mechanics. Improved geodetic techniques applied to subduction zones have also revealed the role that other deformation processes play through the seismic cycle, including coseismic (e.g., during the earthquake) deformation, and afterslip and viscoelastic deformation in the years and decades following major earthquakes (Johnson and Tebo, 2018; Li et al., 2018a; Sun et al., 2014).

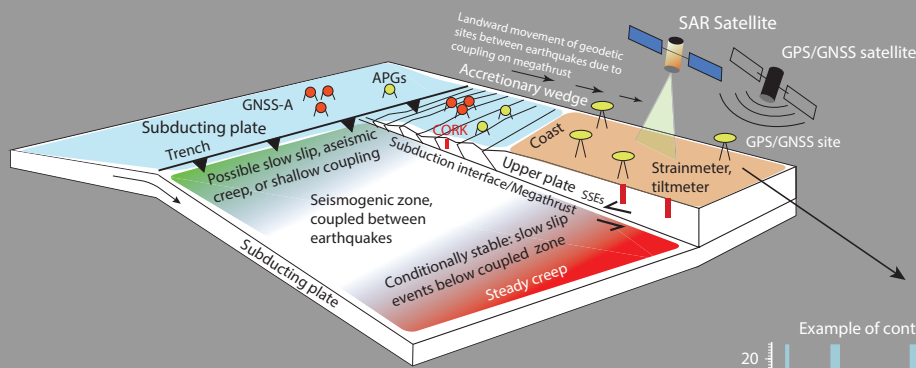
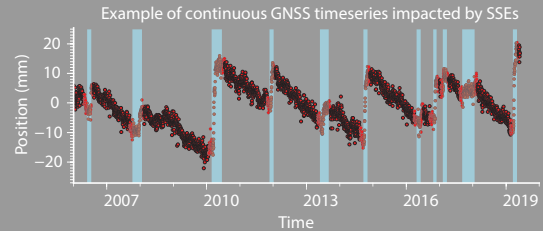


Figure 1. Schematic diagram illustrating the types of geodetic measurements that can be made at subduction zones to discern megathrust coupling and slip behavior. Lower right panel shows an example of a continuous GPS/GNSS site timeseries impacted by slow slip event (SSE) occurrence (SSE timing illustrated with shaded blue bars). This schematic is highly generalized, and there are many examples globally where the nature of slip behavior is far more heterogeneous in the various regions than shown.



## Methods used to evaluate subduction locking and slip behavior

GPS/GNSS measurements are taken at survey points permanently attached to the ground either by intermittent (campaign- or survey-style) or continuous (daily) collection of phase and pseudorange data from the constellation of GPS/GNSS satellites that orbit the Earth. Campaign-style measurements lack temporal resolution as measurements are typically undertaken months to years apart for several days at a time, so are largely suitable for investigating long-term deformation rates in a region over many years. Continuously operating onshore GPS/GNSS networks have become increasingly common at subduction zones and other plate boundaries worldwide, enabling extraction of daily or sub-daily positions of these sites with millimeter-level accuracy. High-rate, real-time positioning of continuous GPS/GNSS sites has also contributed to rapid seismological characterization of earthquakes (Crowell et al., 2012), and is currently being used to develop geodetic earthquake early warning systems (Ruhl et al., 2017). High-rate data can also help characterize the earthquake rupture process (Miyazaki et al., 2004) and strong ground motion characteristics (Grapenthin et al., 2018). Continuously operating GPS/GNSS networks positioned above subduction zones in Canada and Japan led to the first discoveries of episodic slow slip events, lasting weeks to years (Dragert et al., 2001; Hirose et al., 1999). Interferometric Synthetic Aperture Radar (InSAR) techniques have also become widely used to resolve coseismic and postseismic deformation processes at subduction zones (Beavan et al., 2011; Lin et al., 2013) as well as some slow slip events (Bekeart et al., 2015; Hamling and Wallace, 2015). As InSAR relies on repeated satellite images of the Earth's surface, it provides much greater spatial coverage (albeit with reduced temporal coverage) than GPS/GNSS, or other techniques that utilize instruments that are typically widely spaced (>20 km). Borehole instrumentation, such as strainmeters, tiltmeters, and pore pressure sensors as a proxy for volumetric strain at onshore and offshore at subduction zones are proving increasingly useful to reveal transient

slip behavior (Araki et al., 2017; Davis et al., 2015; Hawthorne and Rubin, 2013; Obara et al., 2004), with much greater sensitivity than either GPS/GNSS or InSAR methods. On the seafloor, GPS/GNSS-Acoustic methods, which involve acoustic ranging using a ship or a Wave Glider on the sea surface that is precisely located by GPS/GNSS satellites, are capable of detecting centimeter-level horizontal deformation rates (Bürgmann and Chadwell, 2014). Absolute Pressure Gauges, which measure vertical deformation of the seafloor by continuously recording changes in pressure due to the overlying water column are becoming widely used to resolve centimeter-level vertical deformation offshore during earthquakes and slow slip events (Ito et al., 2013; Wallace et al., 2016).

Many modelling techniques that connect geodetic displacements to locking and/or slip on a megathrust plate boundary assume that the Earth's crust largely behaves as an elastic medium. The majority of fault slip models developed to fit surface geodetic data assume that this behavior can be captured with dislocations in an elastic, half-space, for which widely used analytical equations have been developed (e.g., Okada, 1992). To address locking at subduction zones, a “backslip” approach (Savage, 1983) is the most widely used, which assumes slip in a direction opposite to that of plate motion to determine the elastic component of deformation due to locking. To capture the complex kinematics and active tectonics of some subduction settings, many have turned to elastic block modelling to discern interseismic coupling, where the velocity field is fit by rotation of elastic crustal blocks, and backslip along those block boundaries (e.g., McCaffrey, 2002). This approach has been implemented at a number of subduction margins worldwide (La Femina et al., 2009; Loveless and Meade, 2010; McCaffrey et al., 2000; Nishimura et al., 2018; Schmalz et al., 2014; Wallace et al., 2004). Although such elastic models have proven very useful, they are limited in their ability to address the influence of other rheologies on crustal deformation at subduction zones such as viscoelasticity, recognized as an important aspect of deformation during the earthquake cycle (Wang et al., 2012). They can also have a large impact on interseismic coupling results (Li et al., 2015; 2018a).

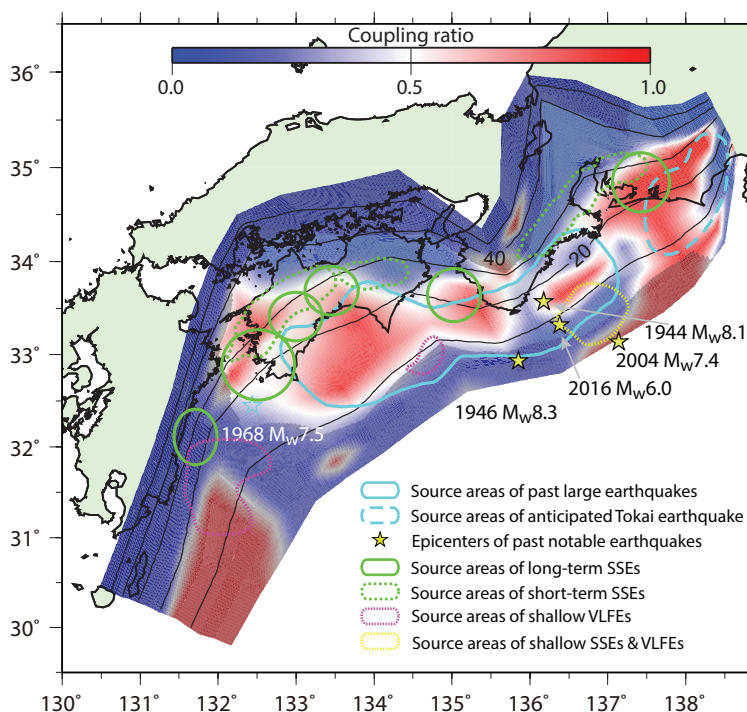
To investigate transient slip events (episodic slow slip events, and afterslip following earthquakes), elastic dislocation methods are also commonly used, by inverting surface displacements to estimate slip on faults embedded in an elastic half-space. Time-dependent inversions fitting continuous GPS/GNSS timeseries - as opposed to models fitting static displacement fields - enable more thorough exploration of the evolution of these slip events. A number of codes with a variety of different approaches and assumptions have been developed to undertake time-dependent inversions for transient deformation (e.g., Segall and Matthews, 1997; Miyazaki et al., 2006; McCaffrey, 2009; Kositsky and Avouac, 2010).

## Geodetic insights into megathrust slip processes at MARGINS and GeoPRISMS sites

Geodetic investigations of crustal deformation at subduction margins provide important context for efforts that use other techniques (seismic imaging, earthquake seismology, heat flow, electromagnetics, geochemistry, rock deformation experimental studies, among others) to constrain the physical controls on subduction megathrust slip behavior. In particular, previous and ongoing geodetic studies at MARGINS and GeoPRISMS focus sites have provided important underpinning datasets to inform strategies for scientific targets and data acquisition efforts, to answer key questions such as: What governs the size, location and frequency of great subduction zone earthquakes and how is this related to the spatial and temporal variation of slip behaviors observed along subduction faults? How does deformation across the subduction plate boundary evolve in space and time, through the seismic cycle and beyond? <http://geoprisms.org/initiatives-sites/scd/>. Although some of the geodetic studies summarized here were undertaken by international partners, or through funding from other NSF programs (or other federal agencies), they have all contributed greatly to broader outcomes of MARGINS and GeoPRISMS at each of the focus sites.

The Philippine Sea Plate is subducting westward beneath southwest Japan along the Nankai Trough at rates of  $\sim 6$  cm/yr (DeMets et al., 2010). This subduction zone has a long, well-established history of producing Great earthquakes ( $M_w > 8.0$ ), approximately every 90-260 years, with the latest of these being the 1944  $M \sim 8.0$  Tonankai earthquake and the 1946  $M \sim 8.2$  Nankaido earthquake (Ando, 1975). Numerous geodetic studies indicate that the subduction interface at the Nankai Trough is currently interseismically coupled in the source region of these great earthquakes (Mazzotti et al., 2000; Nishimura et al., 2018; Yokota et al., 2016, among others; Fig. 2), suggesting that the currently accruing elastic strain will ultimately be relieved in future megathrust earthquakes. Although most interseismic deformation models are based on data from an extensive network of land-based continuous GPS/GNSS stations (Sagiya et al., 2000), Japan has also led the world in acquiring data from a network of about 15 GPS/GNSS-Acoustic arrays overlying the offshore Nankai Trough, providing the first-ever detailed view of horizontal deformation related to interseismic coupling on an plate boundary offshore (Yokota et al., 2016). Together, the onshore and offshore data suggest that the down-dip limit of interseismic coupling occurs at  $\sim 30$  km depth beneath Shikoku Island and the Kii Peninsula, and locking persists up to 0-10 km depth (Nishimura et al., 2018; Yokota et al., 2016; Fig. 2). Moreover, repeated levelling and tide gauge datasets acquired since 1947 have revealed variations in rates of vertical deformation through different stages of the seismic cycle, highlighting the influence of viscoelastic mantle flow on the deformation field for several decades following major earthquakes there (Johnson and Tebo, 2018). These rich and long-lived onshore and offshore geodetic datasets has made the Nankai Trough one of the best-instrumented subduction zones on the planet, enabling characterization of crustal deformation processes throughout the megathrust seismic cycle.

Figure 2. Geodetic coupling ratio, SSEs, and past subduction earthquakes at the Nankai Trough subduction zone, southwest Japan (from Nishimura et al., 2018). Solid blue lines represent source regions of 1946 Nankai and 1944 Tonankai earthquakes. Dashed blue lines represent the suggested source region for Tokai earthquake. Solid and dotted green lines represent source regions of long-term slow slip events (SSEs) and short-term SSEs (see Nishimura et al., 2018 for source of SSE and earthquake locations). Dotted yellow lines represent source regions of very low frequency earthquakes (VLFs) determined by National Research Institute for Earth Science and Disaster Resilience. Stars represent epicenters of notable earthquakes. Contours on subduction interfaces are isodepths at 10 km intervals.

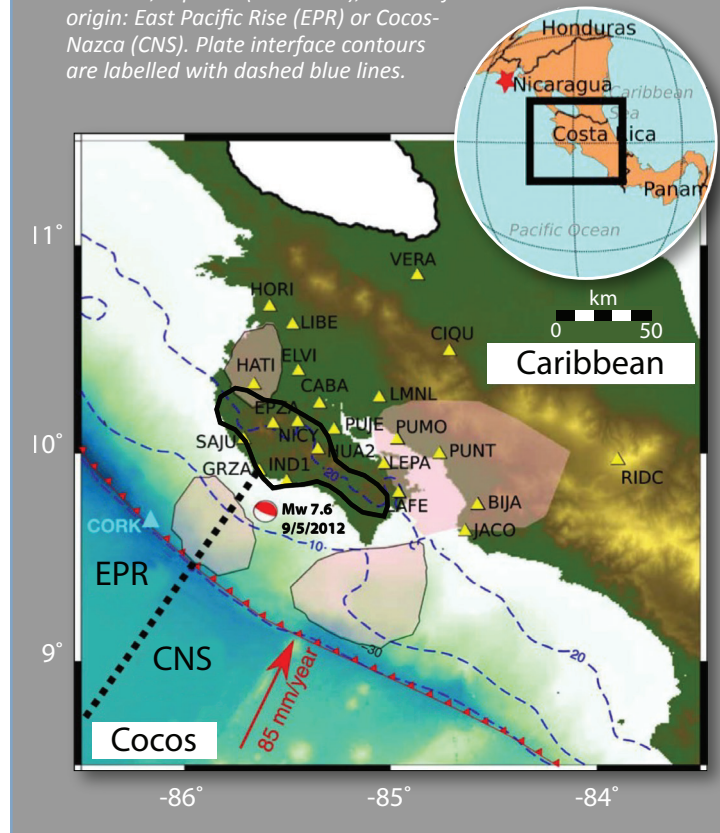


The Nankai Trough is also the site of a diverse range of SSEs and related seismic phenomena (tremor, low-frequency earthquakes), that shed further light on seismic cycle processes on the megathrust (Obara and Kato, 2016). The most well-known of these are Episodic Tremor and Slip (ETS) events, which involve abundant seismic tremor accompanied by small SSEs (~1-3 cm of inferred slip) detected by borehole tiltmeters (Obara et al., 2004) and continuous GPS/GNSS networks (Nishimura et al., 2013), largely occurring below the locked seismogenic zone in the down-dip transition from brittle to ductile deformation (Fig. 2). There are also long-term SSEs lasting a few years in the Tokai region, down-dip of inferred interseismic coupling (Ohta et al., 2004; Miyazaki et al., 2006; Ozawa et al., 2012), as well as approximately one-year-long SSEs in the Bungo Channel (Hirose et al., 1999), in the along-strike transition from deep coupling at the Nankai Trough to an aseismic creep-dominated margin offshore Kyushu (Fig. 2). These long-term SSEs appear to recur less frequently, approximately every five to six years in the case of the Bungo Channel SSEs (Kobayashi and Yamamoto, 2011). More recently, pore pressure changes detected in borehole observatories offshore in the Nankai Trough have revealed episodic SSEs (that often coincide with very low frequency earthquakes and tremor) near the trench, up-dip of the seismogenic zone (Araki et al., 2017). These offshore SSEs may accommodate 30-55% of the overall plate motion near the trench (Araki et al., 2017), consistent with interseismic coupling coefficients on the megathrust of less than 50% from offshore GPS/GNSS-A arrays (Nishimura et al., 2018; Fig. 2). The offshore Nankai Trough SSEs are the first that have been clearly observed up-dip of a deeply locked seismogenic zone known to produce Great (Mw >8.0) subduction earthquakes. Episodic SSEs are thought to occur on faults where the frictional properties straddle the boundary from seismic (velocity weakening) to aseismic (velocity strengthening) behavior, and the location of these shallow, offshore SSEs could signify the up-dip limit of the seismogenic zone at Nankai.

#### COSTA RICA'S MIDDLE AMERICA TRENCH

Along Costa Rica's Middle American Trench the oceanic Cocos plate subducts beneath the continental Caribbean plate at a rate of ~8.5-9 cm/yr (DeMets et al., 2010). This rapid rate of convergence is responsible for generating magnitude 7+ earthquakes about every fifty years (1853, 1900, 1950 and 2012) beneath the Nicoya Peninsula, the northwestern margin of the Costa Rica subduction zone. Due to the advantageous location of the Nicoya Peninsula extending seaward over the seismogenic zone, the regularity of large earthquakes, and its timing late in the earthquake cycle, Costa Rica was one of the first regions chosen as a focus site for the MARGINS Program. With MARGINS' support, dense campaign and continuous GPS/GNSS and regional seismic observations covering the Nicoya Peninsula began in 1999 and continue today. These two decades of instrumental coverage captured the most recent Mw 7.6 earthquake on September 5, 2012, allowing the late interseismic, co-seismic and postseismic phases of the earthquake cycle to be well-recorded (Fig. 3). These data have been used to construct models of the interseismic strain accumulation on the plate interface (Feng et al., 2012; Xue et al., 2015; Kyriakopoulos et al., 2016), the distributions of

Figure 3. Summary map of the slip behavior of the northern Costa Rica margin. The focal mechanism marks the epicenter of the 9/5/2012 Mw 7.6 earthquake with the black solid contour indicating the region with mainshock slip greater than 1 m. This contour corresponds well to the area of maximum interseismic strain accumulation. The major slow slip patches are shown in the salmon color and occur up and down-dip of the locked seismogenic zone. Current GPS/GNSS stations (yellow triangles) and the CORK borehole with the pressure sensor (cyan triangle) used to determine the slow slip distribution are indicated. The Cocos and Caribbean Plates are labeled along with their convergence direction, slip rate (red arrow), and seafloor origin: East Pacific Rise (EPR) or Cocos-Nazca (CNS). Plate interface contours are labelled with dashed blue lines.



co-seismic slip (Yue et al., 2013; Protti et al., 2014; Liu et al., 2015; Kyriakopoulos et al., 2016) and afterslip (Malservisi et al., 2015), and the timing and location of slow slip and tremor events (Walter et al., 2011, 2013; Dixon et al., 2014).

Geodetic observations during the late interseismic phase identified a region of slip deficit that tightly encompassed the subsequent rupture area of the 2012 Nicoya earthquake (e.g., Feng et al., 2012; Protti et al., 2014). This highlights the importance of making GPS/GNSS observations during the interseismic phase to identify the likely location of asperities in future earthquakes. In addition to hosting large earthquakes every 50 to 60 years, large slow-slip events (~Mw 7.0) and seismic tremor activity have been observed every 2-3 years. These large regular SSEs have slip both up and down-dip of the locked seismogenic zone, while smaller SSEs occur more frequently with most of their slip constrained to shallow (<15 km) depths (Dixon et al., 2014). Areas that experienced significant slow slip prior to the 2012 earthquake did not experience seismic rupture in the 2012 mainshock.

If this behavior is characteristic of other subduction zones, it suggests that better monitoring of SSEs could provide useful information for earthquake and tsunami forecasting. Due to the close proximity of the Nicoya Peninsula to the trench (~70-90 km), shallow SSEs are well-recorded on near-shore GPS/GNSS stations, but the addition of deformation signals recorded on borehole pressure sensors (Davis et al., 2011, 2015) and fluid flow meters (Brown et al., 2005) near the trench has allowed more detailed models of offshore slow slip to be constructed. These models reveal shallow slow slip that propagates all the way to the trench and that may trigger second subevents at depth (Davis et al., 2015; Jiang et al., 2017). Exactly how slow slip cycles evolve with time around the locked seismogenic zone is not known and awaits the accumulation of data from future SSEs.

#### CASCADIA SUBDUCTION ZONE

In the Cascadia subduction zone, offshore the Pacific Northwest region of the U.S. and Canada, the Juan de Fuca plate subducts obliquely under North America at a rate of approximately 3-4 cm/year, generally increasing in rate from south to north (Fig. 4). This subduction zone features characteristic large earthquakes every few hundred years (Goldfinger et al., 2012) with very few earthquakes on the plate interface between these large events. The last such event was a full margin rupture that occurred on January 16, 1700 with a magnitude of approximately 9.0 (Atwater et al., 2015). Goldfinger et al. (2012) estimate a roughly four in ten chance of an earthquake rupturing the southern part of the Cascadia subduction zone over the next fifty years, with a likely magnitude of approximately 8.0. The same study also estimates a one in ten chance of a full margin rupture similar to the 1700 event over the same time frame. This represents a significant risk to the cities of Portland, OR and Seattle, WA and surrounding areas. A number of studies over the past two decades, many funded by the MARGINS and GeoPRISMS programs, have furthered our understanding of the mechanics of the Cascadia subduction zone and what future earthquakes may look like here.

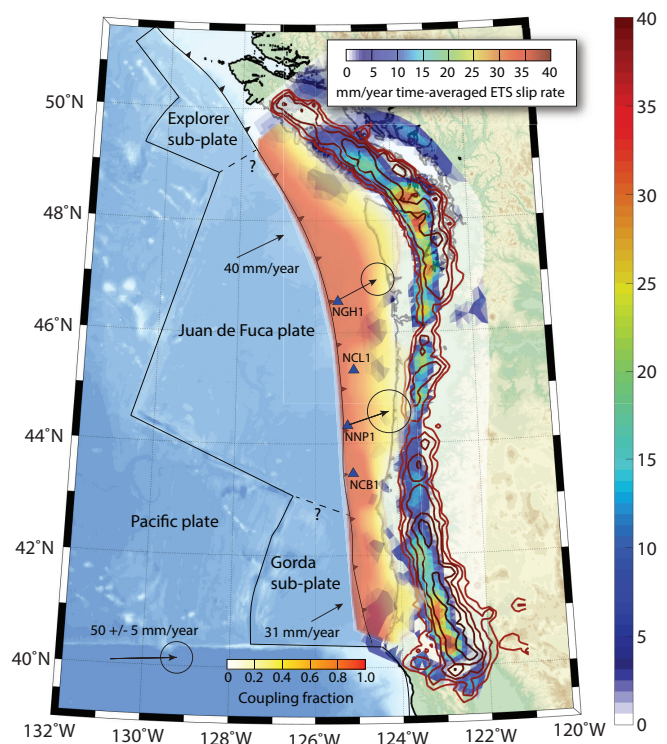
Geodetic studies in Cascadia are complicated by other tectonic signals, such as the rotation of the forearc blocks relative to North America. Multiple interseismic coupling models created from onshore GPS/GNSS data exist with some variation between them (e.g. Schmalzle et al., 2014; Pollitz and Evans, 2017; Li et al., 2018a). Figure 4 features one of the coupling models from Schmalzle et al., 2014. Most models broadly agree on a strongly coupled zone located mainly offshore. An offshore rupture of the region of high coupling inferred from geodesy is consistent with paleoseismic observations of land subsidence during the 1700 earthquake (Wang et al., 2013).

Figure 4. Summary of Cascadia interseismic coupling and episodic tremor and slip (ETS). Red to yellow colors indicate the degree of coupling from onshore GPS/GNSS data, assuming strong coupling at the trench (Schmalzle et al., 2014). Rainbow colors indicate the time-averaged slip rate on the plate interface attributable to ETS events (Bartlow et al., 2020). Brown lines are contours of tremor density from the Pacific Northwest Seismic Network catalog (Wech, 2010). Blue triangles indicate the location of GPS/GNSS-Acoustic sites. NNP1 and NGH1 are the original GeoPRISMS funded sites, with preliminary velocities and uncertainties shown (Chadwell et al., 2018).

Onshore GPS/GNSS data in southern Cascadia was also recently used to identify the new phenomenon of dynamically triggered changes in plate interface coupling caused by offshore earthquakes (Materna et al., 2019).

The shallow extent of offshore coupling is very poorly constrained by onshore geodetic instrumentation (Schmalzle et al., 2014), which includes GPS/GNSS sites and borehole strainmeters. Measuring the degree of coupling near the trench is extremely important for constraining both earthquake and tsunami hazards, with a higher degree of shallow coupling leading to greater potential for near-trench coseismic rupture and tsunamigenesis. This requires seafloor geodetic techniques, most importantly through installation of GPS/GNSS-Acoustic sites. GPS/GNSS-Acoustic sites are also important for studying offshore displacement in future earthquakes in Cascadia once they occur (Saunders and Haas, 2018). Four GPS/GNSS-Acoustic sites now exist along the offshore portion of the Cascadia subduction zone, two of which were installed with GeoPRISMS funding (Fig. 4). Measuring shallow coupling with this technique takes a number of years, and full results are not yet available. Preliminary data from the two GeoPRISMS funded sites appear consistent with a moderate-to-large degree of coupling extending to the shallow part of the subduction interface, implying significant tsunami hazard (Chadwell et al., 2018; Fig. 4).

Similar to the Nankai subduction zone, the Cascadia subduction zone hosts abundant ETS events (Rogers and Dragert, 2003), in which tectonic tremor and geodetically observed slow slip migrate together along the subduction zone (Bartlow et al., 2011; Wech and Bartlow, 2014). The ETS events appear to occur not on the down-dip edge of the strongly coupled zone as might be expected by simple frictional models, but rather are located deeper, with a gap of little to no coupling between the strongly coupled zone and the ETS zone (Fig. 4; Hyndman et al., 2015; Bartlow, 2020).



This indicates that ETS behavior is controlled not only by a simple transition from a coupled plate interface to a freely sliding interface, but also by other physical property changes. The most likely candidate is the presence of high pore fluid pressure in the ETS zone, leading to very low effective normal stress, thereby altering the frictional behavior of the interface in this region (Audet et al., 2009; Hyndman et al., 2015; Gao and Wang, 2017). The influence of the ETS events on the timing of great earthquakes in Cascadia is still a topic of scientific debate and warrants further study (e.g., Mazzotti and Adams, 2004; Beeler et al., 2014).

#### THE ALASKA/ALEUTIAN SUBDUCTION ZONE

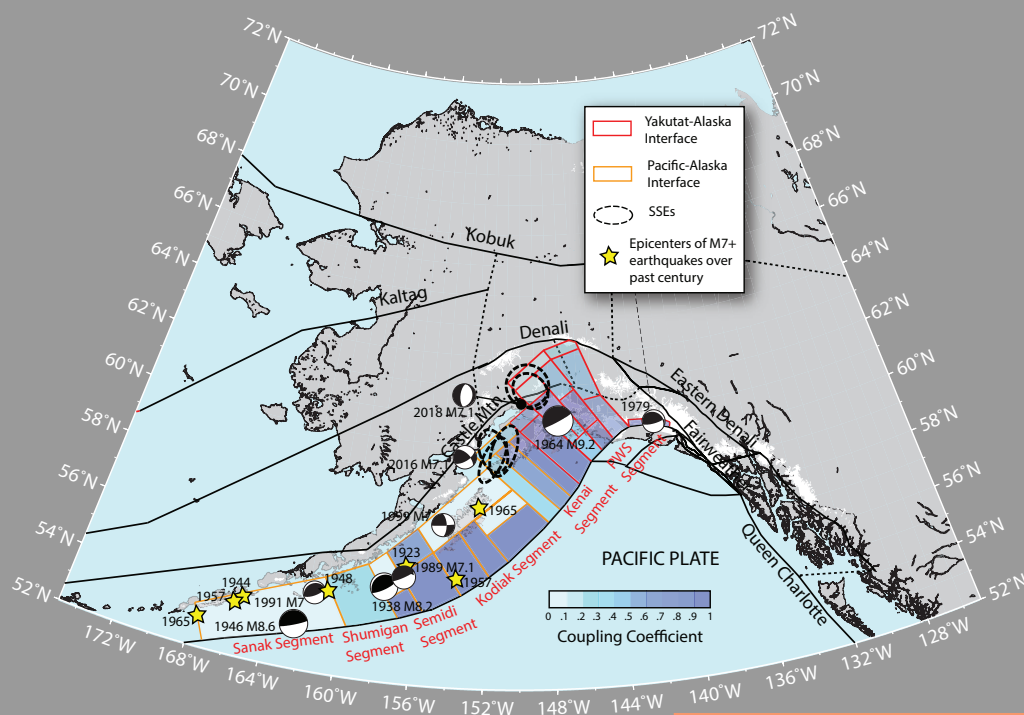
The Alaska-Aleutian subduction zone stretches from the Bering Glacier in the Gulf of Alaska west to the Kamchatka Peninsula. Over the majority of its 4000-km length, the boundary accommodates subduction of the Pacific plate. At its eastern end, however, flat-slab subduction of the Yakutat Block, an oceanic plateau, occurs. This flat-slab region generated the second-largest earthquake recorded, the 1964 Mw 9.2 Prince William Sound earthquake. The earthquake caused extensive regional damage and generated a tsunami that resulted in casualties in Oregon and California and damage as far away as Hawaii. Other sections of the interface have generated five Mw7.9+ earthquakes over the past century along with two Mw7+ intraslab events (Fig. 5).

Geodetic evaluation of interseismic coupling along the Alaska-Aleutian subduction zone is complicated by a number of tectonic and non-tectonic transient signals, including glacial isostatic adjustment, ongoing postseismic deformation from several earthquakes

including the 1964 event, and SSEs. Elastic block modeling of GPS/GNSS data that takes these effects into account reveals a highly variable pattern of coupling along the interface and complicated upper plate motion (Fig. 5). The upper plate rotates counterclockwise throughout south central Alaska before transitioning to increasingly arc-parallel motion through the Alaska Peninsula and the Aleutians as crust is extruded westward into the Bering Sea region (Cross and Freymueller, 2008; Li et al., 2016; Elliott and Freymueller, 2020). Strong coupling occurs beneath Prince William Sound and outboard of Kodiak Island (Li et al., 2016; Elliott and Freymueller, 2020). These areas experienced very high slip during the 1964 earthquake (e.g. Holdahl and Sauber, 1994; Ichinose et al, 2007). Areas that slipped less during the 1964 event appear to be partially coupled or creeping in the present day. This suggests that asperities may persist through multiple earthquake cycles. West of the 1964 rupture, the Shumagin section of the interface, a GeoPRISMS study area, is partially coupled while regions further to the west are creeping (Fournier and Freymueller, 2007; Li et al., 2018; Elliott and Freymueller, 2020).

As mentioned above, SSEs occur along the Alaska subduction zone. Two events have been geodetically documented to the northwest of Prince William Sound (Ohta et al., 2006; Fu et al., 2015) while three have been observed at the western end of the Kenai Peninsula (Wei et al., 2012; Li et al., 2016; Fig. 5). All of these SSEs were multi-year events, with one lasting at least nine years (Li et al., 2016) and occur in relatively weakly coupled sections of the interface down-dip of more strongly coupled areas. The observed SSEs are located near and on either side of the transition between the Yakutat flat slab and more “normal” Pacific crust.

Figure 5. Summary map of slip behavior along the Alaska subduction zone. PWS is Prince William Sound. A coupling coefficient of 0 indicates a fully creeping fault segment while a coefficient of 1 indicates a fully coupled fault accumulating strain at the full relative plate motion rate. Fault geometries and coupling distribution from Elliott and Freymueller (2020). SSE locations from Li et al. (2016), Ohta et al. (2006), Fu et al. (2015), and Wei et al. (2012). Earthquake locations and focal mechanisms from Estabrook et al. (2000), Estabrook et al. (1994), Lopez and Okal (2006), Kanamori (1970), and the Alaska Earthquake Center database, and the U.S. Geological Survey/Earthquake Hazards Program catalog.



All of the geodetic observations discussed above were from land-based GPS/GNSS sites at least 100 km from the trench, leading to poor resolution of coupling along the shallowest regions of the subduction zone. As part of a recently funded GeoPRISMS project, three seafloor GPS/GNSS-Acoustic sites were established in the weakly coupled Shumagin segment and the adjacent strongly coupled Semidi segment (Chadwell et al., 2018). The new geodetic data will help resolve the transition between strong and weak coupling and determine if and how coupling varies between the up-dip and down-dip sections of the segment.

#### NEW ZEALAND'S HIKURANGI SUBDUCTION ZONE

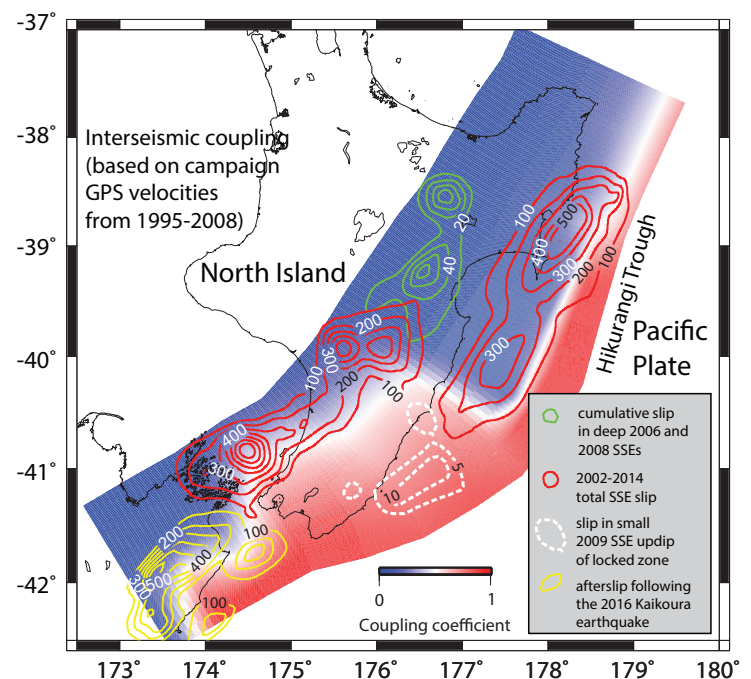
The Hikurangi subduction zone accommodates westward subduction of the Pacific Plate beneath the East Coast of the North Island of New Zealand, along the Hikurangi Trough. It continues north of New Zealand to link up to the Kermadec and Tonga subduction zones; the southern termination of the subduction zone is not well-defined, but likely occurs somewhere in the northern South Island. Extensive campaign GPS/GNSS datasets have been acquired at the onshore portion of this margin since the mid-1990's (Beavan et al., 2016) and have revealed the distribution of interseismic coupling on the plate interface below (Darby and Beavan, 2001; Wallace et al., 2004, 2012). Elastic block modeling of interseismic GPS/GNSS velocities show that the southern Hikurangi subduction interface undergoes deep (25-40 km) interseismic coupling, while further north this transitions to a mostly creeping plate boundary (Fig. 6).

Numerous SSEs have been observed on the Hikurangi subduction zone by continuous GPS/GNSS sites in the region, operated by GeoNet (Gale et al., 2015; [www.geonet.org.nz](http://www.geonet.org.nz)). They occur at a large range of depths with widely varying duration, recurrence, and magnitude characteristics (Bartlow et al., 2014; Wallace and Beavan, 2010; Wallace, 2020). SSEs at the northern and central Hikurangi margin largely occur off the east coast and tend to be shallow (<15 km depth), relatively frequent (every 1-2 years), and are short in duration--lasting a few to several weeks. A deployment of seafloor Absolute Pressure Gauges (APGs) at the offshore northern Hikurangi margin suggest 1-5 cm of uplift of the seafloor during a 2014 SSE indicating that these shallow SSEs propagate close to the trench (Wallace et al., 2016). More recently, GeoPRISMS has supported additional APG and GPS/GNSS-A deployments offshore New Zealand, which captured a recent, large SSE at the central

Hikurangi margin in mid-2019. SSEs at southern Hikurangi are deep (50-20 km), less frequent (4-5 year recurrence intervals), and typically last a year or more. In general, the spatial pattern of SSE occurrence tracks along the edges of interseismic coupling at the southern and central Hikurangi margin, while SSEs offshore the east coast occupy the apparently mostly creeping portion of the central and northern plate boundary (Fig. 6).

New Zealand's historical record is relatively short (~170 years), and no great (Mw>8.0) earthquakes on the Hikurangi subduction zone have been recorded. The largest recorded subduction thrust events were two Mw ~7.2 earthquakes in 1947, that ruptured the shallow, mostly creeping plate boundary offshore Gisborne, and generated large tsunamis (8-10 m) (Doser and Webb, 2003; Downes et al., 2000). However, paleoseismic evidence suggests that the currently locked southern Hikurangi margin (Fig. 6) ruptures every ~300-800 years (Clark et al., 2019), and there is also evidence for coastal subsidence consistent with great subduction earthquakes at the offshore central Hikurangi margin (which currently appears to creep and undergo episodic slow slip) (Hayward et al., 2016). Despite the limitations of the historical subduction earthquake record, intriguing interplays between SSEs and recent earthquakes in New Zealand have been widely observed. The most spectacular of these interactions was widespread triggering of slow slip in most of New Zealand's slow slip regions following the 2016 Mw 7.9 Kaikoura earthquake, including distant (~600 km) dynamically triggered SSEs at the northern Hikurangi subduction zone (Wallace et al., 2017, 2018). Investigation of these triggered SSEs was partially supported under a GeoPRISMS funded project. Triggering of slow slip events have been observed in other Hikurangi margin earthquakes (Francois-Holden et al., 2008; Koulali et al., 2017), and some New Zealand earthquakes of Mw 6.0-7.1 may also have been triggered by SSEs (Koulali et al., 2017; Wallace et al., 2014, 2017).

Figure 6. Interseismic coupling based on campaign GPS velocities (1995-2008), shown in terms of interseismic coupling coefficient ( $\phi_{ic}$ ; Wallace et al., 2012). Where  $\phi_{ic} = 0$  then this region of the fault is creeping at the full long-term slip rate and if  $\phi_{ic} = 1$  there is no creep in the interseismic period. In the case where  $\phi_{ic}$  is neither 0 nor 1, one could interpret it as a spatial and/or temporal average of creeping and non-creeping patches. Contours represent different periods of cumulative SSE slip (green, red, white) or afterslip (yellow) on the subduction interface (see key for explanation). Figure modified from Wallace (2020).



## Discussion

Together, the GeoPRISMS and MARGINS focus sites have encompassed a wide variety of subduction zones with a range of physical characteristics and megathrust slip behavior. A number of factors have been suggested to influence slip behavior at subduction zones, including thermal state/incoming plate age (Hyndman et al., 1997), geometric and/or lithological heterogeneity of the plate boundary fault (Wang and Bilek, 2014; Barnes et al., 2020), sediment thickness on the subducting plate (Ruff, 1989), upper plate crustal properties (Bassett and Watts, 2015), metamorphic phase changes (Peacock and Hyndman, 1999; Moore and Saffer, 2001), and the influence of fluid pressure on effective stress (Kitajima and Saffer, 2012; Saffer and Tobin, 2011). Cascadia and Nankai are two excellent examples of warm, thickly sedimented (>1 km thick) subduction zones, and indeed, they exhibit many similar slip characteristics including deep interseismic coupling, evidence for past Great subduction earthquakes, and some of the strongest associations between tectonic tremor and SSEs observed anywhere. Alaska is the site of strong along-strike variations in plate age, dip, and incoming sediment thickness/plate roughness, as well as large along-strike variations in megathrust slip behavior and locking, making it an excellent locale to investigate the physical controls on slip behavior. Likewise, the Hikurangi margin (a cold subduction zone endmember), is the site of a large along-strike variation in sediment thickness and incoming plate roughness, and upper plate properties that change in tandem with variations in interseismic coupling and slow slip distributions. The Middle America Trench in Costa Rica is an excellent example of a thinly sedimented, geometrically rough, and a moderately young incoming plate age (~15-25 Ma) that exhibits highly heterogeneous seismic and aseismic slip processes.

Taken as a whole, regions with low coupling or highly heterogeneous coupling (e.g., Costa Rica, north Hikurangi, the Shumagins, and offshore Kyushu southwest of the Nankai Trough; Figs. 2-6) coincide with areas of rough crust subduction, suggesting that a geometrically and lithologically heterogeneous plate interface may promote creep, slow slip events, and/or heterogeneous coupling (Wang and Bilek 2014; Barnes et al., 2020). In contrast, the deeply and more uniformly locked Cascadia, Nankai, southern Hikurangi, and the Prince William Sound/Kenai Peninsula area of Alaska are all the site of thick incoming sediment packages. These parallels suggest that incoming plate properties may play an important role in determining geodetically observed slip behavior. Many other changes in characteristics of these margins exist, such as upper plate structure/properties, the location of thermally controlled metamorphic phase transitions, inferred variations in fluid pressure, and many other properties that also show associations with different types of slip behavior. The challenge in the near-term will be to better integrate and evaluate these observations (and those from other subduction zones) to discern the primary controls on megathrust slip behavior and earthquakes.

Geodetically inferred interseismic coupling in Costa Rica, Alaska and Nankai coincide with the rupture areas of well-documented historical earthquakes, while regions of strong coupling in Cascadia

and Hikurangi coincide with prehistoric earthquake ruptures inferred from paleoseismological investigations. These suggest that contemporary geodetic coupling estimates are a useful guide to locations of future subduction megathrust ruptures, with important implications for seismic and tsunami hazard. However, we cannot rule out seismic rupture (and tsunamigenesis) in regions that appear to be dominated by aseismic creep and SSE processes, as was observed during a pair of Mw 7.2 earthquakes near the trench offshore the northern Hikurangi in 1947. The 1947 earthquakes produced tsunamis of 8-10 m, and are widely considered to be “tsunami earthquakes”, where the tsunami that was generated was much larger than expected based on the earthquake magnitude. The conditional frictional stability thought to be present in shallow SSE zones may also make these portions of the subduction interface favorable for hosting tsunami earthquakes (Bilek and Lay, 2002). It is also possible that regions of strong geodetic locking may vary over time as the physical properties that control it change. However, resolving locking variations over a single to multiple seismic cycles, or determining if it is persistent over many seismic cycles in most locations requires sustained geodetic and seismological monitoring at subduction margins globally.

Shallow (<15 km depth) SSEs are observed in Costa Rica, north Hikurangi, and the Nankai Trough. In all three cases, these are relatively short in duration (less than one month), and occur relatively frequently (every 1-2 years). Long-term (>1 year), deep (>25 km depth), less frequent (every 5 years or more) SSEs have been observed at Nankai (Bungo Channel and Tokai SSEs), Alaska, Costa Rica, and southern Hikurangi. This contrast in some shallow vs. deep SSE characteristics suggest fundamentally different physical conditions or deformation mechanisms may be at play in deep versus shallow SSE regions. Numerical models based on rate and state friction are able to produce deep, long SSES and shallow, short SSEs with higher effective normal stress in the deep SSE regions compared to the shallow regions (Shibazaki et al., 2019). Higher effective normal stress in deep SSE regions is not unexpected given the greater overburden in the deep SSE regions, and may provide one explanation for these differences in shallow vs. deep SSE characteristics. However, deep ETS events observed at Nankai and Cascadia are shorter (weeks to months), frequent, and more strongly associated with seismic signatures (tremor), suggesting some fundamental differences in physical conditions exist in regions with ETS vs. deep, long-term SSE regions. It is also worth noting that Cascadia and Nankai have a young incoming plate, which may influence metamorphic phase transitions and subsequent fluid release that may play a role in the ETS process (e.g., Fagereng and Diener, 2011).

For the most part, deep SSEs at all of the subduction margins discussed here occur down-dip of the interseismically coupled seismogenic zone. In Cascadia and Nankai, there is thought to be a gap between the down-dip end of coupling and slow slip/tremor regions (Figs. 2 and 4). The reasons for this, and the nature of deformation within this gap are still not well-understood. SSEs in Costa Rica and Hikurangi closely track the edges of the locked seismogenic zone (Figs. 3 and 6). Shallow SSEs at Nankai and Costa

Rica appear to occur up-dip of the seismogenic zone, and may represent the up-dip transition from stick-slip (velocity weakening) behavior to aseismic (velocity strengthening) behavior near the trench. At Hikurangi, Costa Rica, and Cascadia SSE regions appear to be largely creeping over multiple SSE cycles, which suggests all of the elastic strain accumulated between SSEs is relieved during slow slip. It is important to consider the implications of this for seismic hazard: is all of the plate motion in SSE regions accommodated aseismically, leaving little to occur during a large earthquake?

## Future challenges and the way ahead

Our understanding of contemporary slip processes at subduction plate boundaries has been transformed in the last two decades, largely due to the development and maturation of a range of geodetic techniques, and widespread installation of permanent geodetic monitoring networks to monitor crustal deformation. However, scientists are only beginning to piece together the ways in which plate motion is accommodated at subduction zones, at timescales ranging from seconds to hundreds of years, at all stages of the earthquake cycle. Significant gaps in our knowledge remain, particularly with regards to the behavior of offshore subduction megathrusts, spatiotemporal variation in slip processes throughout the earthquake cycle (and the influence of this on future earthquake occurrence), and the role of inelastic rheologies on deformation throughout the earthquake cycle.

Offshore portions of subduction zones pose the greatest tsunami hazard and also represent our largest observational gap—widespread application of robust techniques to measure seafloor and subseafloor crustal deformation represents our most challenging frontier. GeoPRISMS has helped to embark on this new frontier by facilitating new seafloor geodetic experiments in Alaska, Cascadia, and New Zealand, utilizing both GPS/GNSS-Acoustic arrays and Absolute Pressure Gauges for horizontal and vertical (respectively) seafloor deformation. Offshore scientific drilling initiatives (through the International Ocean Discovery Program) have installed subseafloor observatories at Nankai, Costa Rica, New Zealand, and Cascadia, enabling high-fidelity detection of near-trench transient deformation, while scientists in Japan have amassed an impressive array of seafloor geodetic data along their subduction zones. Although the MARGINS and GeoPRISMS focus sites are more advanced in the acquisition of offshore geodetic data than most other subduction margins, more offshore geodetic infrastructure is needed in these locations and at subduction zones elsewhere if we are to unravel the nature of deformation near the trench and the implications of this for tsunami hazard.

Major gaps also exist in our knowledge of deformation throughout the earthquake cycle and how this evolves through time. Addressing this requires a concerted effort to obtain long (decades and beyond), uninterrupted timeseries of crustal deformation at numerous subduction zones, both onshore and offshore, and underscores the importance of continuing to operate continuous GPS/GNSS networks and other existing geodetic and seismological infrastructure. Tantalizing evidence for pre-seismic transients leading-up to the Mw 9.0 Tohoku-Oki earthquake in northern

Japan (Mavrommatis et al., 2014) and elsewhere (Bedford et al., 2020) suggest the possibility several years to months-long changes in deformation rates at subduction zones may presage major ruptures, with important societal implications. However, determining what constitutes a precursor (or not) requires building-up a large number of such observations in many subduction environments. Long geodetic records spanning all phases of the seismic cycle will help to address the role of viscoelastic deformation at different stages in the seismic cycle, and the influence of this on the megathrust strain accumulation and release processes. Advancing our understanding of deformation at all stages of the earthquake cycle also requires us to move beyond widely used elastic half-space models, and account for the influence of both inelastic and anelastic rheologies and spatial variability in crustal elastic properties.

The discovery of episodic slow slip events has opened our eyes to the highly transient nature of slip and locking on subduction megathrusts. However, significant gaps exist in our ability to detect smaller, shorter transient events below the resolution limits of more commonly used geodetic techniques. More widespread use of highly sensitive tiltmeters, strainmeters, and borehole pressure sensors will help to reveal the full spectrum of deformation processes, and bridge the gap between seismologically observed deformation phenomena (e.g., seconds to minutes) and those observed geodetically. Offshore subduction zones are a particularly attractive target for these activities as they offer opportunities for very near-field monitoring, within a few kilometers of the fault. Evidence is also mounting that significant transience in interseismic coupling processes may exist, including spatiotemporal variations in coupling within the locked seismogenic zone on short (weeks to months) timescales (e.g., Haines et al., 2019), increased coupling induced by nearby earthquakes (e.g., Materna et al., 2019), and pre-seismic unlocking in the years prior to large megathrust events (Mavrommatis et al., 2014). Making more headway on detecting these “coupling transients” (and resolving the processes that produce them) requires improvements in data analysis and modelling techniques, sustaining and building on existing GPS/GNSS infrastructure, and development of low-noise instrumentation capable of detecting longer-term changes (months to years) in crustal deformation. Development of efficient modelling approaches to more robustly address uncertainties in coupling and slip distribution on megathrusts is also needed.

Although geodetic observations can provide critical insights into the varied modes of slip behavior on megathrusts, integration of these observations with a range of geophysical, geological, laboratory, and modelling studies are required to resolve the underlying physical processes. Programs like MARGINS and GeoPRISMS have enabled focused, multi-disciplinary efforts at several subduction zones, producing great advances in our ability to bridge the gap between observation and process. Future programs, such as the SZ4D initiative, will help to ensure continued progress in this societally important area of research, and generate new discoveries regarding the physical processes underpinning our planet’s largest earthquake and tsunami factories. ■

# References

- Ando, M. (1975). Source mechanisms and tectonic significance of historical earthquakes along the Nankai Trough, Japan. *Tectonophysics*, 27, 119-140
- Araki, E., D.M. Saffer, A. Kopf, L.M. Wallace, T. Kimura, Y. Machida, S. Ide (2017). Recurring and triggered slow slip events near the trench at the Nankai Trough subduction megathrust. *Science*, 356, 1157-1160, doi: 10.1126/science.aan3120
- Atwater, B.F., S. Musumi-Rokkaku, K. Satake, Y. Tsuji, K. Ueda, D.K. Yamaguchi (2015) *The orphan tsunami of 1700—Japanese clues to a parent earthquake in North America*. 2nd ed.: Seattle, University of Washington Press, U.S. Geol Survey Professional Paper 1707, 135 p
- Audet, P., M.G. Bostock, N.I. Christensen, S.M. Peacock (2009). Seismic evidence for overpressured subducted oceanic crust and megathrust fault sealing. *Nature*, 457, 7225, 76-78
- Barnes, P.M. et al. (2020). Slow slip source characterized by lithological and geometric heterogeneity. *Science Advances*, 6, 13, eaay3314, DOI: 10.1126/sciadv.aay3314
- Bartlow, N.M., S.I. Miyazaki, A.M. Bradley, P. Segall (2011). Space-time correlation of slip and tremor during the 2009 Cascadia slow slip event. *Geophys Res Lett*, 38, 18
- Bartlow, N.M., L.M. Wallace, R.J. Beavan, S. Bannister, P. Segall (2014). Time-dependent modeling of slow slip events and associated seismicity and tremor at the Hikurangi subduction zone, New Zealand. *J Geophys Res: Solid Earth*, 119, 1, 734-753
- Bartlow, N.M. (2020). A long-term view of episodic tremor and slip in Cascadia. *Geophys Res Lett*, 47, 3, e2019GL085303
- Bassett, D., A.B. Watts (2015) Gravity anomalies, crustal structure, and seismicity at subduction zones: 2. Interrelationships between fore-arc structure and seismogenic behavior. *Geochem Geophys*, 16, doi:10.1002/2014GC005685
- Beavan, J., S. Samsonov, P. Denys, R. Sutherland, N. Palmer, M. Denham, (2011b). Oblique slip on the Puysegur subduction interface in the 2009 July Mw 7.8 Dusky Sound earthquake from GPS and InSAR observations: implications for the tectonics of southwestern New Zealand. *Geophys J Int*, 183, 1265-1286
- Beavan, J., L. Wallace, N. Palmer, P. Denys, S. Ellis, N. Fournier, S. Hreinsdottir, C. Pearson, M. Denham (2016). New Zealand GPS velocity field: 1995-2013. *New Zealand J Geol Geophys*, doi: 10.1080/00288306.2015.1112817.
- Bedford, J., M. Moreno, Z. Deng, O. Oncken, B. Schurr, T. John, J.C. Baez, M. Bevis (2020), Months-long, thousand kilometre scale wobbling before great subduction earthquakes. *Nature*, 580, 628-636
- Beeler, N.M., E. Roeloffs, W. McCausland (2014). Re-estimated effects of deep episodic slip on the occurrence and probability of great earthquakes in Cascadia. *Bull Seismol Soc Am*. 104, 1, 128-144
- Bekaert, D., A. Hooper, T. Wright, (2015). Reassessing the 2006 Guerrero slow slip event, Mexico: Implications for large earthquakes in the Guerrero Gap. *J Geophys Res: Solid Earth*, 120, 2, 1357-1375
- Bilek, S.L. T. Lay (2002). Tsunami earthquakes possibly widespread manifestations of frictional conditional stability. *Geophys Res Lett*, 29, 18-1-18-4.
- Brown, K.M., M.D. Tryon, H.R. DeShon, L.M. Dorman, S.Y. Schwartz (2005). Correlated transient fluid pulsing and seismic tremor in the Costa Rica subduction zone. *Earth Planet Sci Lett*, 238, 1, 189-203
- Bürgmann, R., D. Chadwell (2014). Seafloor geodesy. *Ann Rev Earth Planet Sci*, 42, 509-534
- Chadwell, C.D., D.A. Schmidt, S.C. Webb, S.L. Nooner, T.L. Erickson, B.A. Brooks, J.H. Foster (2018), Expansion of GPS-acoustic arrays offshore the Cascadia and Alaska subduction zones, Abstract T44C-02, 2018 AGU Fall Meeting
- Clark, K., J. Howarth, N. Litchfield, U. Cochran, J. Turnbull, L. Dowling, A. Howell, K. Berryman, F. Wolfe (2019). Geological evidence for past large earthquakes and tsunamis along the Hikurangi subduction margin, New Zealand. *Mar Geol*, 412, 139-172
- Cross, R.S., J.T. Freymueller (2008). Evidence for and implications of a Bering plate based on geodetic measurements from the Aleutians and western Alaska. *J Geophys Res*, 113, B07405, doi:10.1029/2007JB005136
- Crowell, B.W., Y. Bock, D. Melgar (2012). Real-time inversion of GPS data for finite fault modeling and rapid hazard assessment. *Geophys Res Lett*, 39, L09305, doi:10.1029/2012GL051318
- Darby, D., J. Beavan (2001). Evidence from GPS measurements for contemporary interplate coupling on the southern Hikurangi subduction thrust and for partitioning of strain in the upper plate. *J Geophys Res*, 106, 30,881-30,891, doi:10.1029/2000JB000023
- Davis, E., M. Heeseman, K. Wang (2011). Evidence for episodic aseismic slip across the subduction seismogenic zone off Costa Rica: CORK borehole pressure observations at the subduction prism toe. *Earth Planet Sci Lett*, 306, 3-4, 299-305, doi:10.1016/j.epsl.2011.04.017
- Davis, E.E., H. Villinger, T. Sun (2015). Slow and delayed deformation and uplift of the outermost subduction prism following ETS and seismogenic slip events beneath Nicoya Peninsula, Costa Rica. *Earth Planet Sci Lett*, 410, 117-127
- DeMets, C., R.G. Gordon, D.F. Argus (2010). Geologically current plate motions. *Geophys J Int*, 181, 1-80
- Dixon, T.H., Y. Jiang, R. Malservisi, R. McCaffrey, N. Voss, M. Protti, V. Gonzalez (2014). Earthquake and tsunami forecasts: Relation of slow slip events to subsequent earthquake rupture. *Proc Nat Acad Sci*, 114, 17,039-17,044
- Doser D.I., Webb T.H. (2003). Source parameters of large historical (1917-1961) earthquakes, North Island, New Zealand. *Geophys J. Int*, 152, 795-832
- Downes, G., T.H. Webb, M.J. McSaveney, C. Chague-Goff, D.J. Darby, A. Barnett (2000). The March 25 and May 17 1947 Gisborne earthquakes and tsunamis: Implication for tsunami hazard for East Coast, North Island, New Zealand, paper presented at Joint IOC/IUGG International Workshop: Tsunami Risk Assessment Beyond 2000—Theory, Practice and Plans, Intergovt Oceanogr Comm, Moscow, 14-16 June
- Dragert, H., W. Kelin, T.S. James (2001). A silent slip event on the deeper Cascadia subduction interface. *Science*, 292, 1525-1528
- Elliott, J., J.T. Freymueller (2020). A block model of present-day kinematics of Alaska and Western Canada. *J Geophys Res: Solid Earth*, 124, doi.org/10.1029/2019JB018378
- Estabrook, C.H., K.H. Jacob, L.R. Sykes (1994). Body wave and surface wave analysis of large and great earthquakes along the Eastern Aleutian Arc, 1923-1993: Implications for future events. *J Geophys Res*, 99, B6, 11643-11662, doi:10.1029/93JB03124
- Fagereng, Å., J.F.A. Diener (2011). Non-volcanic tremor and discontinuous slab dehydration. *Geophys Res Lett*, 38, L15302, doi:10.1029/2011GL048214
- Feng, L., A.V. Newman, M. Protti, V. González, Y. Jiang, T.H. Dixon (2012). Active deformation near the Nicoya Peninsula, northwestern Costa Rica, between 1996 and 2010: Interseismic megathrust coupling. *J Geophys Res*, 117, doi:10.1029/2012JB009230
- Francois-Holden, C., et al. (2008). The MW 6.6 Gisborne Earthquake of 2007: Preliminary records and general source characterisation. *Bull NZ Soc Earthquake Eng*, 41, 4, 266-277
- Fournier, T. J., J.T. Freymueller (2007). Transition from locked to creeping subduction in the Shumagin region, Alaska. *Geophys Res Lett*, 34, L06303, doi:10.1029/2006GL029073
- Fu, Y., Z. Liu, J.T. Freymueller (2015). Spatiotemporal variations of the slow slip event between 2008 and 2013 in the southcentral Alaska subduction zone. *Geochem Geophys*, 16, 7, 2450-2461, doi.org/10.1002/2015GC005904
- Gale, N.K., M. Gledhill, L. Chadwick, L. Wallace (2015). The Hikurangi margin continuous GNSS and seismograph network of New Zealand. *Seismol Res Lett*, 86, 1, doi:10.1785/0220130181
- Gao, X., K. Wang (2017). Rheological separation of the megathrust seismogenic zone and episodic tremor and slip. *Nature*, 543, 7645, 416-419
- Goldfinger, C., et al. (2012). Turbidite event history - Methods and implications for Holocene paleoseismicity of the Cascadia subduction

- zone: U.S. Geological Survey Professional Paper 1661–F, 170p. <https://pubs.usgs.gov/pp/pp1661f/>
- Grapenthin, R., M. West, C. Tape, M. Gardine, J. Freymueller (2018). Single-frequency instantaneous GNSS velocities resolve dynamic ground motion of the 2016 Mw 7.1 Iniskin, Alaska, earthquake. *Seismol Res Lett*, 89, 3, 1040-1048, doi.org/10.1785/0220170235
- Haines, J., L.M. Wallace, L. Dimitrova (2019). Slow slip event detection in Cascadia using vertical derivatives of horizontal stress rates. *J Geophys Res Solid Earth*, 124, doi.org/10.1029/2018JB016898
- Hamling, I.J., L.M. Wallace (2015). Silent triggering: Aseismic crustal faulting induced by a subduction slow slip event. *Earth Planet Sci Lett*, 421, 13-19
- Hawthorne, J.C., A.M. Rubin (2013). Short-time scale correlation between slow slip and tremor in Cascadia. *J Geophys Res Solid Earth*, 118, 1316-1329
- Hayward, B.W., H.R. Grenfell, A.T. Sabaa, U.A. Cochran, K.J. Clark, L. Wallace, A.S. Palmer (2016). Salt marsh foraminiferal record of 10 large Holocene (last 7500 yr) earthquakes on a subducting plate margin, Hawkes Bay, New Zealand. *Geol Soc Am Bull*, doi:10.1130/B31295.1
- Hirose, J., K. Hirahara, F. Kimata, N. Fjii, S. Miyazaki (1999). A slow thrust slip event following the two 1996 Hyuganada earthquakes beneath the Bungo Channel, southwest Japan. *Geophys Res Lett*, 26, 3237-3240
- Holdahl, S.R., J. Sauber (1994). Coseismic slip in the 1964 Prince William Sound earthquake: A new geodetic inversion. *Pure Appl Geophys*, 142, 55-82, doi:10.1007/BF00875968
- Hyndman, R.D., M. Yamano, D.A. Oleskovich (1997). The seismogenic zone of subduction thrust faults. *Isl Arc*, 6, 244-260, doi:10.1111/j.1440-1738.1997.tb00175.x
- Hyndman, R.D., P.A. McCrory, A. Wech, H. Kao, J. Ague (2015). Cascadia plate fluids channelled to fore-arc mantle corner: ETS and silica deposition. *J Geophys Res Solid Earth*, 120, 4344-4358, doi:10.1002/2015JB011920
- Ichinose, G., P. Somerville, H.K. Thio, R. Graves, D. O'Connell (2007). Rupture process of the 1964 Prince William Sound, Alaska, earthquake from the combined inversion of seismic, tsunami, and geodetic data. *J Geophys Res*, 112, B07306, doi:10.1029/2006JB004728
- Ito, Y., et al. (2013). Episodic slow slip events in the Japan subduction zone before the 2011 Tohoku-Oki earthquake. *Tectonophysics*, 600, 14-26
- Jiang, Y., Z. Liu, E.E. Davis, S.Y. Schwartz, T.H. Dixon, N. Voss, R. Malservisi, M. Protti (2017). Strain release at the trench during shallow slow slip: The example of Nicoya Peninsula, Costa Rica. *Geophys Res Lett*, 44, 4846-4854, doi 10.1002/2017GL072803
- Johnson, K., D. Tebo (2018). Capturing 50 years of postseismic mantle flow at Nankai Subduction zone. *J Geophys Res*, 123, 11, 10,091-10,106, doi.org/10.1029/2018JB016345
- Kanamori, H. (1970). The Alaska Earthquake of 1964: Radiation of long-period surface waves and source mechanism. *J Geophys Res*, 75, 26, 5029-5040, doi:10.1029/JB075i026p05029
- Kitajima, H., D.M. Saffer (2012). Elevated pore pressure and anomalously low stress in regions of low frequency earthquakes along the Nankai Trough subduction megathrust. *Geophys Res Lett*, 39, 23, L23301, doi.org/10.1029/2012GL053793
- Kobayashi, A., T. Yamamoto (2011). Repetitive long-term slow slip events beneath the Bungo Channel, southwestern Japan, identified from leveling and sea level data from 1979 to 2008. *J Geophys Res*, 116, B04406, doi:10.1029/2010JB007822
- Kositsky, A.P., J.-P. Avouac (2010). Inverting geodetic time series with a principal component analysis-based inversion method. *J Geophys Res*, 115, B03401, doi:10.1029/2009JB006535
- Koulali, A., S. McClusky, L. Wallace, S. Allgeyer, P. Tregoning, E. D'Anastasio, R. Benavente (2017). Slow slip events and the 2016 Te Araroa Mw 7.1 earthquake interaction: Northern Hikurangi subduction, New Zealand. *Geophys Res Lett*, 44, doi:10.1002/2017GL074776
- Kyriakopoulos, C., A.V. Newman (2016). Structural asperity focusing, locking, and earthquake slip along the Nicoya megathrust, Costa Rica. *J Geophys Res Solid Earth*, 121, 5461-5476, doi: 10.1002/2016JB012886
- LaFemina, P., T.H. Dixon, R. Govers, E. Norabuena, H. Turner, A. Saballos, G. Mattioli, M. Protti, W. Strauch (2009). Fore-arc motion and Cocos Ridge collision in Central America. *Geochem Geophys*, 10, Q05S14, doi:10.1029/2008GC002181
- Li, S., J. Freymueller, R. McCaffrey (2016). Slow slip events and time-dependent variations in locking beneath Lower Cook Inlet of the Alaska-Aleutian subduction zone. *J Geophys Res Solid Earth*, 121, 1060-1079, doi:10.1002/2015JB012491
- Li, S., M. Moreno, J. Bedford, M. Rosenau, O. Oncken (2015). Revisiting viscoelastic effects on interseismic deformation and locking degree: A case study of the Peru-North Chile subduction zone. *J Geophys Res Solid Earth*, 120, 4522-4538, doi:10.1002/2015JB011903
- Li, S., K. Wang, Y. Wang, Y. Jiang, S.E. Dosso (2018). Geodetically inferred locking state of the Cascadia megathrust based on a viscoelastic Earth model. *J Geophys Res Solid Earth*, 123, 8056-8072, doi.org/10.1029/2018JB015620
- Li, S., J.T. Freymueller (2018). Spatial variation of slip behavior beneath the Alaska Peninsula along Alaska-Aleutian subduction zone. *Geophys Res Lett*, 45, 3454-3460, doi.org/10.1002/2017GL076761
- Lin, Y.N., A. Sladen, F. Ortega-Culaciati, M. Simons, J.-P. Avouac, E.J. Fielding (2013). Coseismic and postseismic slip associated with the 2010 Maule Earthquake, Chile: Characterizing the Arauco Peninsula barrier effect. *J Geophys Res: Solid Earth*, 118, 3142-3159, doi:10.1002/jgrb.50207
- Liu, C., Y. Zheng, X. Xiong, R. Wang, A. López, J. Li (2015). Rupture processes of the 2012 September 5 Mw 7.6 Nicoya, Costa Rica earthquake constrained by improved geodetic and seismological observations. *Geophys J Int*, 203, 1, 175-183, doi:10.1093/gji/ggv295
- Lopez, A.M., E.A. Okal (2006). A Seismological Reassessment of the source of the 1946 Aleutian 'tsunami' earthquake. *Geophysical Journal International*, 165, 3, 835-849, doi.org/10.1111/j.1365-246X.2006.02899.x
- Loveless, J.P., B.J. Meade (2010). Geodetic imaging of plate motions, slip rates, and partitioning of deformation in Japan. *J Geophys Res*, 115, B02410, doi:10.1029/2008JB006248
- Loveless, J.P., B.J. Meade (2011). Spatial correlation of interseismic coupling and coseismic rupture extent of the 2011 MW = 9.0 Tohoku-oki earthquake. *Geophys Res Lett*, 38, L17306, doi:10.1029/2011GL048561
- Malservisi, R., et al. (2015). Multiscale postseismic behavior on a megathrust: The 2012 Nicoya earthquake, Costa Rica. *Geochem Geophys*, doi:10.1002/2015GC005794
- Materna, K., N. Bartlow, A. Wech, C. Williams, R. Bürgmann (2019). Dynamically triggered changes of plate interface coupling in Southern Cascadia. *Geophys Res Lett*, 46, 12890- 12899, doi.org/10.1029/2019GL084395
- Mavrommatis, A.P., P. Segall, K.M. Johnson (2014). A decadal-scale deformation transient prior to the 2011 Mw 9.0 Tohoku-oki earthquake. *Geophys Res Lett*, 41, 4486-4494, doi:10.1002/2014GL060139
- Mazzotti, S., J. Adams (2004). Variability of near-term probability for the Next Great Earthquake on the Cascadia Subduction Zone. *Bull Seismol Soc Am*, 94, 5, 1954-1959
- Mazzotti, S., X. Le Pichon, P. Henry, S. Miyazaki (2000). Full interseismic locking of the Nankai and Japan-west Kurile subduction zones: An analysis of uniform elastic strain accumulation in Japan constrained by permanent GPS. *J Geophys Res*, 105, B6, 13,159-13,177
- McCaffrey, R., M.D. Long, C. Goldfinger, P.C. Zwick, J.L. Nabelek, C.K. Johnson, C. Smith (2000). Rotation and plate locking at the southern Cascadia subduction zone. *Geophys Res Lett*, 27, 3117-3120
- McCaffrey, R. (2002). Crustal block rotations and plate coupling, in *Plate Boundary Zones*, Geodyn. Ser., 30, edited by S. Stein and J. Freymueller, 100-122, AGU, Washington, D.C
- McCaffrey, R. (2009). Time-dependent inversion of three-component continuous GPS for steady and transient sources in northern Cascadia. *Geophys Res Lett*, 36, L07304, doi:10.1029/2008GL036784
- Métois, M., C. Vigny, A. Socquet (2016). Interseismic coupling, megathrust earthquakes, and seismic swarms along the Chilean subduction zone (38°-18°S). *Pure Appl Geophys*, 173, 1431-1449
- Miyazaki, S., K.M. Larson, K. Choi, K. Hikima, K. Koketsu, P. Bodin, J. Haase, G. Emore, A. Yamagiwa (2004). Modeling the rupture process of the 2003 September 25 Tokachi-Oki (Hokkaido) earthquake using 1-Hz GPS data. *Geophys Res Lett*, 31, L21603, doi:10.1029/2004GL021457

- Miyazaki, S., P. Segall, J.J. McGuire, T. Kato, Y. Hatanaka (2006). Spatial and temporal evolution of stress and slip rate during the 2000 Tokai slow earthquake. *J Geophys Res*, 111, B03409, doi:10.1029/2004JB003426
- Moore, J.C., D. Saffer (2001). Updip limit of the seismogenic zone beneath the accretionary prism of southwest Japan: An effect of diagenetic to low-grade metamorphic processes and increasing effective stress. *Geology*, 29, 2, 183-186, doi:10.1130/0091-7613
- Nishimura, T., T. Matsuzawa, K. Obara (2013). Detection of short-term slow slip events along the Nankai Trough, southwest Japan, using GNSS data. *J Geophys Res Solid Earth*, 118, 3112-3125, doi:10.1002/jgrb.50222
- Nishimura, T., Y. Yokota, K. Tadokoro, T. Ochi (2018). Strain partitioning and interplate coupling along the northern margin of the Philippine sea plate, estimated from global navigation satellite system and global positioning system-acoustic data. *Geosphere*, 14, 2, 535, doi.org/10.1130/GES01529.1
- Obara, K., H. Hirose, F. Yamamizu, K. Kasahara (2004). Episodic slow slip events accompanied by non-volcanic tremors in southwest Japan subduction zone. *Geophys Res Lett*, 31, L23602, doi:10.1029/2004GL020848
- Obara, K., A. Kato (2016). Connecting slow earthquakes to huge earthquakes. *Science*, 353, 6296, 253-257, doi:10.1126/science.aaf1512
- Ohta, Y., F. Kimata, T. Sagiya (2004). Reexamination of the interplate coupling in the Tokai region, central Japan, based on the GPS data in 1997–2002. *Geophys Res Lett*, 31, L24604, doi:10.1029/2004GL021404
- Ohta, Y., J.T. Freymueller, S. Hreinsdóttir, H. Suito (2006). A large slow slip event and the depth of the seismogenic zone in the south central Alaska subduction zone. *Earth Planet Sci Lett*, 247, 108-116
- Okada, Y. (1992). Internal deformation due to shear and tensile faults in a half-space. *Bull Seismol Soc Am*, 82, 1018-1040
- Ozawa, S., M. Murakami, M. Kaidzu, T. Tada, Y. Hatanaka, H. Yarai, T. Nishimura (2002). Detection and monitoring of ongoing aseismic slip in the Tokai region, central Japan. *Science*, 298, 1009-1012
- Peacock, S.M., R.D. Hyndman (1999). Hydrous minerals in the mantle wedge and the maximum depth of subduction thrust earthquakes. *Geophys Res Lett*, 26, 16, 2517–2520, doi:10.1029/1999GL900558
- Pollitz, F.F., E.L. Evans (2017). Implications of the earthquake cycle for inferring fault locking on the Cascadia megathrust. *Geophysical Journal International*, 209, 1, 167-185
- Protti, M., V. González, A. Newman, T. Dixon, S. Schwartz, J. Marshall, L. Feng, J. Walter, R. Malservisi, S. Owen (2014). Nicoya earthquake rupture anticipated by geodetic measurement of the locked plate interface. *Nature Geosci*, 7, 117-121
- Rogers, G., H. Dragert (2003). Episodic tremor and slip on the Cascadia subduction zone: The chatter of silent slip. *Science*, 300, 5627, 1942-1943
- Ruff, L.J. (1989). Do trench sediments affect great earthquake occurrence in subduction zones. *Pure Appl Geophys*, 129, 1–2, 263-282, doi:10.1007/BF00874629
- Ruhl, C.J., D. Melgar, R. Grapenthin, R.M. Allen (2017). The value of real-time GNSS to earthquake early warning. *Geophys Res Lett*, 44, 16, 8311-8319
- Saunders, J.K., J.S. Haase (2018). Augmenting onshore GNSS displacements with offshore observations to improve slip characterization for Cascadia subduction zone earthquakes. *Geophys Res Lett*, 45, 12, 6008-6017
- Saffer, D.M., H.J. Tobin (2011). Hydrogeology and mechanics of subduction zone forearcs: Fluid flow and pore pressure. *Ann Rev Earth Planet Sci*, 39, 157-186, doi.org/10.1146/annurev-earth-040610-133408
- Savage, J.C. (1983). A dislocation model of strain accumulation and release at a subduction zone. *J Geophys Res*, 88, 4984-4996
- Sagiya, T., K. Ozawa, M. Ohzono, T. Nishimura, Y. Hoso (2010). Consistency and inconsistency between geodetic and geologic fault slip rates in Central Japan. Abstract T44A-06 2010 AGU Fall Meeting
- Schmalzle, G.M., R. McCaffrey, K.C. Creager (2014). Central Cascadia subduction zone creep. *Geochem Geophys*, 15, 4, 1515-1532
- Schwartz, S.Y., J.M. Rokosky (2007). Slow slip events and seismic tremor at circum-Pacific subduction zones. *Rev Geophys*, 45, RG3004, doi:10.1029/2006RG000208
- Segall, P., M. Matthews (1997). Time dependent inversion of geodetic data. *J Geophys Res*, 102, 22,391–22,409
- Shibasaki, B., L.M. Wallace, Y. Kaneko, I. Hamling, Y. Ito, T. Matsuzawa (2019). Three-dimensional modeling of spontaneous and triggered slow-slip events at the Hikurangi subduction zone, New Zealand. *J Geophys Res Solid Earth*, 124, doi.org/10.1029/2019JB018190
- Sun, T., et al. (2014). Prevalence of viscoelastic relaxation after the 2011 Tohoku-oki earthquake. *Nature*, 514, 84–87
- Wallace, L.M., J. Beavan, R. McCaffrey, D. Darby (2004). Subduction zone coupling and tectonic block rotation in the North Island, New Zealand. *J Geophys Res*, 109, doi:10.1029/2004JB003241
- Wallace, L.M., J. Beavan (2010). Diverse slow slip behavior at the Hikurangi subduction margin, New Zealand. *J Geophys Res*, 115, B12402, doi:10.1029/2010JB007717
- Wallace, L.M., P. Barnes, R.J. Beavan, R.J. Van Dissen, N.J. Litchfield, J. Mountjoy, R.M. Langridge, G. Lamarche, N. Pondard (2012). The kinematics of a transition from subduction to strike-slip : an example from the central New Zealand plate boundary. *J Geophys Res Solid Earth*, doi:10.1029/2011JB008640
- Wallace, L.M., N. Bartlow, I. Hamling, B. Fry (2014). Quake clamps down on slow slip. *Geophys Res Lett*, 41, doi:10.1002/2014GL062367
- Wallace, L.M., S.C. Webb, Y. Ito, K. Mochizuki, R. Hino, S. Henrys, S. Schwartz, A. Sheehan (2016). Slow slip near the trench at the Hikurangi subduction zone. *Science*, 352, 6286, 701-704, doi: 10.1126/science.aaf2349
- Wallace, L.M., Y. Kaneko, S. Hreinsdóttir, I. Hamling, Z. Peng, N. Bartlow, E. D’Anastasio, B. Fry (2017). Large-scale dynamic triggering of shallow slow slip enhanced by overlying sedimentary wedge. *Nat Geosci*, 10, 765-770 doi: 10.1038/ngeo3021
- Wallace, L.M., S. Hreinsdóttir, S. Ellis, I. Hamling, E. D’Anastasio, P. Denys (2018). Triggered slow slip and afterslip on the southern Hikurangi subduction zone following the Kaikōura earthquake. *Geophys Res Lett*, 45, 4710-4718, doi.org/10.1002/2018GL077385
- Wallace, L.M. (2020). Slow Slip Events in New Zealand. *Ann Rev Earth Planet Sci*, doi.org/10.1146/annurev-earth-0717190055104
- Walter, J.I., S.Y. Schwartz, M. Protti, V. Gonzalez (2011). Persistent tremor within the northern Costa Rica seismogenic zone. *Geophys Res Lett*, 38, 1, L01307, doi: 10.1029/2010GL045586
- Walter, J.I., S.Y. Schwartz, M. Protti, V. Gonzalez (2013). The synchronous occurrence of shallow tremor and very low frequency earthquakes offshore of the Nicoya Peninsula, Costa Rica. *Geophys Res Lett*, doi:10.1002/grl.50213
- Wang, K., Y. Hu, J. He (2012). Deformation cycles of subduction earthquakes in a viscoelastic Earth. *Nature*, 484, 327-332, doi.org/10.1038/nature11032
- Wang, K. S.L. Bilek (2014). Invited review paper: fault creep caused by subduction of rough seafloor relief. *Tectonophysics*, 610, 1-24
- Wang, P.-L., S.E. Engelhart, K. Wang, A.D. Hawkes, B.P. Horton, A.R. Nelson, R.C. Witter (2013). Heterogeneous rupture in the great Cascadia earthquake of 1700 inferred from coastal subsidence estimates. *J Geophys Res Solid Earth*, 118, 2460-2473, doi:10.1002/jgrb.50101
- Wei, M., J.J. McGuire, E. Richardson (2012). A slow slip event in the south central Alaska Subduction Zone and related seismicity anomaly. *Geophys Res Lett*, 39, L15309, doi.org/10.1029/2012GL052351
- Wech, A.G. (2010). Interactive tremor monitoring. *Seismol Res Lett*, 81, 4, 664-669
- Wech, A. G., N.M. Bartlow (2014). Slip rate and tremor genesis in Cascadia. *Geophys Res Lett*, 41, 2, 392-398
- Xue, L., S. Schwartz, Z. Liu, L. Feng (2015). Interseismic megathrust coupling beneath the Nicoya Peninsula, Costa Rica, from the joint inversion of InSAR and GPS data. *J Geophys Res Solid Earth*, 120, 5, 3707-3722, doi:10.1002/2014JB011844
- Yokota, Y., T. Ishikawa, S. Watanabe, T. Tashiro, A. Asada (2016). Seafloor geodetic constraints on interplate coupling of the Nankai Trough megathrust zone. *Nature*, 534, 7607, 374-377, doi:10.1038/nature17632
- Yue, H., T. Lay, S. Y. Schwartz, L. Rivera, M. Protti, T.H. Dixon, S. Owen (2013). The 5 September 2012 Costa Rica Mw 7.6 earthquake rupture process from joint inversion of high-rate GPS, strong-motion, and teleseismic P wave data and its relationship to adjacent plate boundary interface properties. *J Geophys Res*, 118, 5453- 5453-5466